Development 135, 3587-3597 (2008) doi:10.1242/dev.028118

PTEN deficiency causes dyschondroplasia in mice by enhanced hypoxia-inducible factor 1α signaling and endoplasmic reticulum stress

Guan Yang, Qiang Sun, Yan Teng, Fangfei Li, Tujun Weng and Xiao Yang*

Chondrocytes within the growth plates acclimatize themselves to a variety of stresses that might otherwise disturb cell fate. The tumor suppressor PTEN (phosphatase and tensin homolog deleted from chromosome 10) has been implicated in the maintenance of cell homeostasis. However, the functions of PTEN in regulating chondrocytic adaptation to stresses remain largely unknown. In this study, we have created chondrocyte-specific *Pten* knockout mice (*Pten*$^{co/co}$*;Col2a1-Cre*) using the Cre-loxP system. Following AKT activation, *Pten* mutant mice exhibited dyschondroplasia resembling human enchondroma. Cartilaginous nodules originated from *Pten* mutant resting chondrocytes that suffered from impaired proliferation and differentiation, and this was coupled with enhanced endoplasmic reticulum (ER) stress. We further found that ER stress in *Pten* mutant chondrocytes only occurred under hypoxic stress, characterized by an upregulation of unfolded protein response-related genes as well as an engorged and fragmented ER in which collagens were trapped. An upregulation of hypoxia-inducible factor 1α (HIF1α) and downstream targets followed by ER stress induction was also observed in *Pten* mutant growth plates and in cultured chondrocytes, suggesting that PI3K/AKT signaling modulates chondrocytic adaptation to hypoxic stress via regulation of the HIF1α pathway. These data demonstrate that PTEN function in chondrocytes is essential for their adaptation to stresses and for the inhibition of dyschondroplasia.

KEY WORDS: PTEN, Dyschondroplasia, ER stress, HIF1α, Knockout mouse

INTRODUCTION

Endochondral ossification, the process by which most mammalian skeletons develop, is a temporally and spatially balanced process. Perichondrial cells, which are progenitors for chondrocytes and osteoblasts, develop to form the articular surface and the bone collar. Chondrocytic progenitors give rise to the four subpopulations of chondrocytes within the growth plate: the resting, proliferating, prehypertrophic and hypertrophic chondrocytes. These chondrocytes are arranged in distinct zones and express specific molecular markers. The differentiation of resting chondrocytes into terminal hypertrophic chondrocytes continues until the replacement of cartilaginous growth plate by mineralized bone is complete. During this process, the proliferation and differentiation of chondrocytes is tightly regulated and synchronously coordinated to form a uniformly arranged growth plate that results in normal skeletal development (Karsenty and Wagner, 2002; Kronenberg, 2003).

Cartilaginous tumors may result from abnormal regulation of the proliferation and differentiation of chondrocytes in the adjoining growth plate. These tumors range from benign lesions, such as enchondromas and osteochondromas, to malignant chondrosarcomas (Brien et al., 1997; Potter et al., 2005). Growth factors, such as bone morphogenetic protein (BMP), platelet-derived growth factor (PDGF) and fibroblast growth factor (FGF), and signaling pathways, such as the mitogen-activated protein kinase (MAPK) pathway, that participate in the course of endochondral ossification have also been implicated in the pathogenesis of cartilaginous tumors (Nakase et al., 2001; Robinson et al., 2001; Sulzbacher et al., 2001). The Indian hedgehog/patched/parathyroid hormone-related peptide (IHH/PTCH/PTHrP) and the hypoxia-inducible factor 1α/vascular endothelial growth factor (HIF1α/VEGF) axes, in particular, have been extensively investigated because of their strong associations with tumor grade and prognosis (Ayala et al., 2000; Kunisada et al., 2002). Within the normal growth plate, PTHrP (PTHLH – Mouse Genome Informatics) and IHH act on their respective receptors, PPR (PTHR1) and PTCH1, to exert a tightly coupled negative-feedback loop that controls the proliferation and onset of hypertrophic differentiation of chondrocytes (Kronenberg, 2003). This feedback loop may be interrupted in cartilaginous tumors (Hopyan et al., 2002; Rozeman et al., 2005; Tiet et al., 2006).

Adaptation to hypoxia is another critical event in numerous pathological and physiological settings, including tumor progression and in the survival of avascular tissues, such as cartilage (Dang et al., 2008; Gordan et al., 2007). The HIF1α/VEGF axis supports chondrocyte survival in the interior growth plate, where oxygen tension is much lower than in the exterior region. In addition, this axis may also modulate chondrocytic size and proliferation, cartilaginous matrix accumulation and blood vessel invasion during endochondral bone formation (Schipani, 2005). Following aberrant growth of cartilaginous tumors, however, activation of the HIF1α/VEGF axis, as assessed by the expression levels of HIF1α and VEGF isoforms, is considered as a marker for malignancy (Kalinski et al., 2006; McGough et al., 2002). Nevertheless, it remains largely unknown whether excessive activation of the HIF1α/VEGF pathway causes cartilaginous tumors or is simply a consequence of overt growth. In addition, the mechanism by which tumors emerge from the developing growth plate remains unclear.

As the only cells residing in cartilage, chondrocytes serve multiple functions during endochondral ossification and may be sensitive to a number of different types of stress (Zuscik et al., 2008). Emerging evidence has highlighted an important role of endoplasmic reticulum (ER) stress in endochondral ossification. Induced ER stress in both primary and immortalized chondrocytes

State Key Laboratory of Proteomics, Genetic Laboratory of Development and Diseases, Institute of Biotechnology, 20 Dongdajie, Beijing 100071, China.

*Author for correspondence (e-mail: yangx@nic.bmi.ac.cn)

Accepted 10 September 2008

has been shown to lead to impaired chondrocyte proliferation, differentiation and apoptosis (Oliver et al., 2005; Yang et al., 2005; Yang et al., 2007). A number of studies have shown that deregulation of ER homeostasis is correlated with malformed skeleton development (chondrodysplasia) caused by mutations in genes encoding extracellular matrix (ECM) proteins (Hashimoto et al., 2003; Ho et al., 2007; Pirog-Garcia et al., 2007; Vranka et al., 2001). Chondrocytes expressing a mutant type-X collagen tolerate ER stress, experience delayed terminal differentiation and exhibit chondrodysplasia (Tsang et al., 2007). A recent study has shown that site-1 protease (S1P; MBTPS1 – Mouse Genome Informatics) is necessary for a specialized ER stress response by chondrocytes that is required for the genesis of normal cartilage (Patra et al., 2007). However, the precise function of the ER stress response in cartilage tumor formation remains largely unknown.

The tumor suppressor PTEN (phosphatase and tensin homolog deleted from chromosome 10) is a lipid phosphatase, the major substrate of which is phosphatidylinositol 3,4,5-triphosphate (PIP3), a secondary messenger generated by phosphatidylinositol-3-kinase (PI3K). Loss of PTEN function leads to an accumulation of PIP3 and an activation of its downstream effectors, acute transforming retrovirus thymoma [AKT; also known as protein kinase B (PKB) and AKT1]. As a serine/threonine protein kinase, AKT phosphorylates key intermediate signaling molecules, including glycogen synthase kinase 3β (GSK3β), murine double minute 2 (MDM2) and mammalian target of rapamycin (mTOR; FRAP1), leading to altered cellular proliferation, differentiation, apoptosis, adhesion and migration (Cully et al., 2006; Waite and Eng, 2002). Germline and somatic mutations of *Pten* have been identified in several hereditary disorders and many sporadic human cancers, such as Cowden disease, glioblastomas, endometrial, prostate and breast cancers. Conditional-knockouts of the *Pten* gene within specific tissues in mice have successfully recapitulated the tumorigenesis of human cancers (Chow and Baker, 2006). Nevertheless, little is known about the roles of PTEN/PI3K/AKT signaling in endochondral ossification.

Recently, Ford-Hutchinson et al. reported that targeted inactivation of PTEN in osteochondroprogenitor cells leads to accelerated chondrocyte differentiation and skeletal overgrowth, suggesting that PTEN is dispensable for endochondral ossification (Ford-Hutchinson et al., 2007). By contrast, the present study provides compelling evidence that loss of PTEN expression in chondrocytes leads to delayed chondrocyte differentiation, which is largely owing to increased ER stress in *Pten* mutant resting chondrocytes. Our results also suggest that PTEN/PI3K/AKT signaling is involved in the growth arrest reactions of chondrocytes to hypoxia.

MATERIALS AND METHODS

Mouse strains

To generate chondrocyte-specific *Pten* knockout mice, mice carrying conditional *Pten* alleles ($Pten^{Co/Co}$) (Backman et al., 2001) were bred with *Col2a1-Cre* transgenic mice in which Cre recombinase is under the control of the cartilage-specific *Col2a1* promoter, limiting its expression primarily to cartilage and perichondrium (Zhang et al., 2005). Animals were handled in accordance with institutional guidelines. Littermates were used in all experiments.

Southern blot

Genomic DNAs were isolated from multiple tissues of a *Pten* mutant mouse at P4. Cartilage tissues were taken from growth plates of the femur, tibia and ribs under a dissecting microscope (Nikon). The DNAs were digested with *Hin*dIII, electrophoresed on a 0.8% agarose gel and transferred to nitrocellulose membrane. *Pten* conditional alleles (4.3 kb) and recombined alleles (7.2 kb) were detected by hybridization with a ^{32}P-labeled probe, the template for which was amplified from mouse genomic DNA by PCR using primers 5′-TTTTGAGACAGGGTCTTGTAT-3′ and 5′-CCCACTGAT-AGTAA AATACTG-3′.

Histology, immunohistochemistry (IHC) and whole-mount tissue immunostaining

The knee joints, shoulder joints or rib cages with the fifth to seventh ribs were fixed in 4% paraformaldehyde at 4°C overnight and decalcified in 5% EDTA in PBS. Paraffin sections (4-6 μm) were cut. Safranine O, von-Kossa method and Hematoxylin and Eosin (H&E) staining were performed as described (Tan et al., 2007). The primary antibodies for IHC were: anti-PTEN (Cell Signaling), anti-phosphorylated AKT (Cell Signaling), anti-Col II (DSHB) and anti-HIF1α (Novus). Sections were counterstained with Hematoxylin or Alcian Blue. TUNEL assay was performed according to the manufacturer's instructions (Chemicon). Anti-CD31 (BD Pharmingen) whole-mount immunostaining was performed by standard procedures (Lan et al., 2007). The percentage of vascularized surface and the total length of vessels within a defined area of the lateral femoral condyles were quantified using Image-Pro Plus (Media Cybernetics).

Electron microscopy

Electron microscopy analysis was performed on P5 growth plate cartilage from shoulder joints or on cultured chondrocytes by standard procedures. Ultrathin sections were stained in uranyl acetate and lead citrate and examined using an EM400 electron microscope (Philips).

In situ hybridization

In situ hybridization was performed on paraffin sections using standard procedures. Probes were labeled with ^{35}S-UTP for *Col10a1*, *Ihh*, *Ppr*, $p21^{Cip1}$, *BiP* and $p57^{Kip2}$, *Pgk* and *Vegf* (Pfander et al., 2004). Slides were dipped in photographic emulsion (Amersham Pharmacia) and exposed for 3-10 days before developing.

BrdU labeling and labeling-chasing assay

Pregnant females or postnatal mice were injected intraperitoneally with 100 μg/g body weight BrdU (Sigma-Aldrich) 1-6 hours before sacrifice. For the long-term labeling-chasing assay, pregnant females with embryos at E15.5 were injected intraperitoneally with 100 μg/g body weight BrdU three times per day for 2 days. For the short-term labeling-chasing assay, pregnant females with embryos at E18.5 were injected intraperitoneally with 100 μg/g body weight BrdU twice in 1 day. Sections of knee joints or shoulder joints were incubated overnight with anti-BrdU antibody (Sigma-Aldrich), and counterstained with Alcian Blue or Hematoxylin after visualization with DAB as the chromogen.

Primary chondrocyte cultures and western blot

Primary chondrocytes were isolated from cartilage of knee joints and rib cages of P2 mice. Briefly, dissected tissues with cartilage were digested in 0.1% collagenase I (Gibco)/DMEM (Hyclone) to remove muscles, ligaments and bone tissue, and in 0.2% collagenase II (Gibco)/DMEM to disperse into single chondrocytes. Pooled chondrocytes were lysed for western blot analyses using antibodies against PTEN (Santa Cruz), phosphorylated AKT (Santa Cruz), HIF1α (Novus), β-actin (Sigma-Aldrich), α-tubulin (Santa Cruz) or CREB1 (Cell Signaling). Pooled chondrocytes were also resuspended and seeded in 6-well dishes (200,000 cells/well) in DMEM/F12 (1:1) medium (Hyclone) supplemented with penicillin/streptomycin (Hyclone) and 10% FCS under normoxia (21% O_2) or hypoxia (2% O_2) conditions for the indicated times. To stabilize HIF1α levels in normoxia, dimethyloxaloylglycine (DMOG) (Cayman Chemicals) was added to the culture medium. Antibodies against HIF1α (Novus), BiP (Cell Signaling) or α-tubulin (Santa Cruz) were employed for western blot analyses.

Northern blot and real-time PCR

Total RNA from cartilage or cultured chondrocytes was extracted using TRIZOL (Invitrogen). Total cellular RNA (10 μg) was loaded in each lane and size fractionated by 1% formaldehyde-agarose gel electrophoresis. Hybridization was performed with a ^{32}P-labeled *Col2a1* probe. Total RNAs were also reverse-transcribed using the mRNA Selective PCR Kit (TaKaRa).

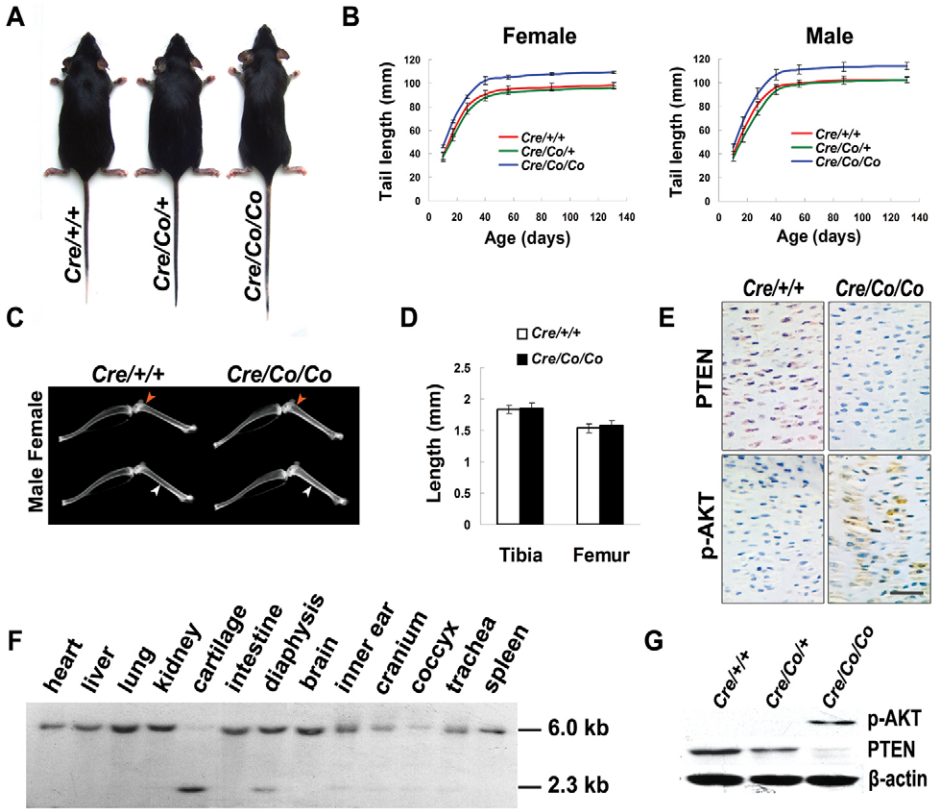

Fig. 1. Targeted disruption of the *Pten* gene in mouse chondrocytes results in skeleton overgrowth. (**A**) Phenotype of *Pten*$^{+/+}$;*Col2a1-Cre* (left), *Pten*$^{Co/+}$;*Col2a1-Cre* (middle) and *Pten*$^{Co/Co}$;*Col2a1-Cre* (right) littermates at P40. (**B**) Tail length measurements of female (left) and male (right) mice at various time points. Each point represents the mean ±s.d. from six mice. (**C**) Soft X-ray images of femur and tibia from P50 mice showing increased width (red arrowheads) and bone density (white arrowheads) of long bones in mutant mice. (**D**) Tibia and femur length were not significantly changed in mutant mice. Mean ±s.d. of eight samples from four mice of each genotype. P>0.05. (**E-G**) Efficient deletion of *Pten* in mutant cartilage as revealed by immunohistochemistry (E), Southern blot (F) and western blot (G). Loss of *Pten* also caused phosphorylation of AKT (p-AKT) within chondrocytes (E,G). Scale bar: 50 μm.

Real-time PCR was repeated at least four times for each gene with the Roche LightCycler 2.0 system using an SYBR Green assay (Sun et al., 2008). Expression values were normalized to *Hprt*. The primer sequences were as follows: *Pgk*, 5′-GGACTTCAACGTTCCTATGAA-3′ and 5′-CCAGCAGAGATTTGAGTTCAG-3′; *Hprt*, 5′-ATGCCGAGGATTTGGAAAAAGTGTTT-3′ and 5′-TGTCCCCCGTTGACTGATCATTACAG-3′. Primer sequences for *Vegf* and its isoforms (*Vegf*$_{120}$, *Vegf*$_{164}$) were as previously described (Maes et al., 2004).

Statistical analysis

Results are presented as mean ± s.d. Statistical differences were determined by Student's *t*-test. Significance was accepted at *P*-values less than 0.05.

RESULTS

Targeted disruption of *Pten* in chondrocytes causes dyschondroplasia

To disrupt the *Pten* gene in chondrocytes, we crossed a mouse strain carrying *Pten* conditional alleles (*Pten*$^{Co/Co}$) (Backman et al., 2001) with *Col2a1-Cre* transgenic mice (Zhang et al., 2005) to generate the *Pten*$^{Co/Co}$;*Col2a1-Cre* mutant. The bodies of newborn mutant mice were longer than those of littermate controls (Fig. 1A). At postnatal day (P) 40, the tails of mutant mice were 11-14% longer than those of *Pten*$^{Co/+}$;*Col2a1-Cre* and *Pten*$^{+/+}$;*Col2a1-Cre* controls (Fig. 1B). Radiographic analyses revealed that the width of mutant long bones was visibly expanded, particularly at the metaphysis (Fig. 1C). The bone density was also increased in mutant mice of both genders, as indicated by reduced radiolucency in cortical and trabecular bones (Fig. 1C). The lengths of the appendicular bones, as represented by the tibia and femur at P50, were not significantly changed in the mutant (Fig. 1D). Almost all the mutant mice developed thoracic kyphosis as they aged, and died before 18 months from progressive paralysis of the hindlimb (data not shown).

PTEN protein can normally be detected in the growth plate chondrocytes, perichondrial cells and periosteal cells. In the mutant tibia, no staining was observed in these cells in either the nucleus or cytoplasm, suggesting efficient deletion of *Pten* (Fig. 1E and data not shown). The loss of PTEN resulted in robust phosphorylation of AKT (p-AKT) in these cells as revealed by immunohistochemistry (IHC) (Fig. 1E and data not shown). Southern blot analysis carried out in a broader range of tissues confirmed that exons 4 and 5 of *Pten* had been deleted by Cre-mediated recombination in tissues containing chondrocytes (inner ear, coccyx and trachea) and osteoblasts (diaphysis and cranium), with the highest efficiency of deletion (95%) observed in purified chondrocytes isolated from knee joints and rib cages (Fig. 1F). The upregulation of p-AKT in *Pten* mutant chondrocytes was further confirmed by western blot analyses (Fig. 1G). These results indicated that *Pten* had been efficiently disrupted in chondrocytes and partially in osteoblasts via *Col2a1-Cre*-mediated recombination.

To characterize in greater detail the skeletal abnormalities in the *Pten*$^{Co/Co}$;*Col2a1-Cre* mice, the proximal femur and tibia of ten mutant mice ranging in age from P30 to P60 were sectioned for histological analysis. A majority of the *Pten* mutant mice exhibited obvious dyschondroplasia. We identified 14 cartilaginous nodules in the epiphyseal cavities of femur from nine mutant mice (Fig. 2B). Four cartilaginous nodules were observed in the bone marrow cavities of the tibia and femur in four of these mutant mice (Fig. 2D,F). These nodules were not found in the tibia and femur of control mice (Fig. 2A,C,E). These cartilaginous neoplasms were singly and asymmetrically distributed in close proximity to the medial aspect of the metaphyseal growth plates of knee joints. Tissues in these nodules were benign and well-differentiated, as characterized by the heterogeneity and diversity in the degree of cellularity of the chondrocytes as compared with those of normal growth plate cartilage

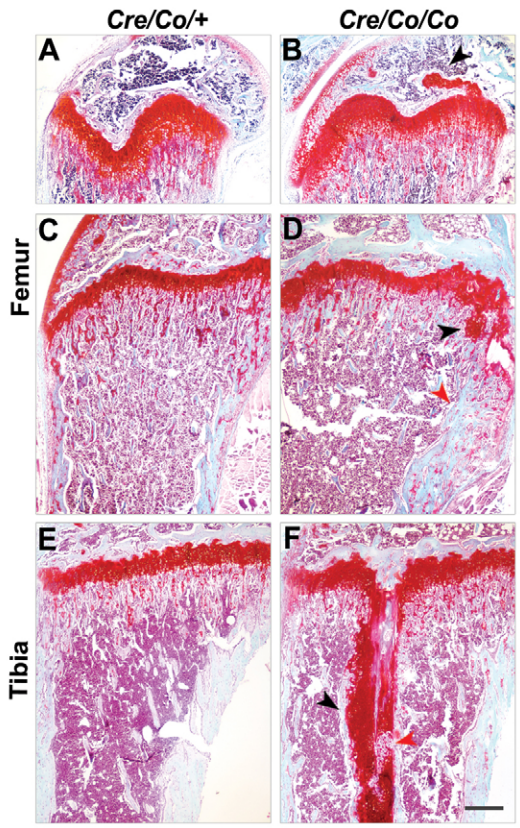

Fig. 2. Dyschondroplasia in adult *Pten*$^{Co/Co}$;*Col2a1-Cre* mice. (**A-F**) Safranine O staining performed on sections of femur (A-D) and tibia (E,F) from control (A,C,E) or mutant (B,D,F) littermates. Cartilaginous nodules were present in the epiphysis (B, black arrowhead), metaphysis (D, black arrowhead) or diaphysis (F, black arrowhead) of long bones in mutant mice. Cartilaginous nodules resulted in ectopic ossification within cortical bone (D, red arrowhead) or within the bone marrow cavity (F, red arrowhead). Age of bones: P32 in A,B; P58 in C,D; P48 in E,F. Scale bar: 500 μm.

(see Fig. S1A,B in the supplementary material). Individual nodules were usually limited at their periphery by a lamella of well-mineralized trabecular bone (see Fig. S1C,D in the supplementary material). Myxoid changes, manifested as a fraying of the matrix, were also seen (see Fig. S1D, asterisk, in the supplementary material). These neoplasms disappeared, coincident with the fusion of the growth plate at 6 months of age. No cartilaginous nodules were found in mutant mice older than 6 months (n=5, data not shown). All these data indicated that the targeted disruption of *Pten* in chondrocytes resulted in benign, early-onset and self-limiting tumor-like lesions in the appendicular bones of young mutant mice.

Aberrant and asynchronous chondrocyte proliferation in the growth plate of *Pten* mutant mice

Tumorigenesis is usually associated with aberrant proliferation, particularly in cases of PTEN deficiency. Therefore, we initially hypothesized that the formation of cartilaginous neoplasms in *Pten* mutant mice would coincide with a cluster of proliferating chondrocytes somewhere within the developing growth plates. However, as judged by BrdU incorporation, no significant differences were observed between mutant and control growth plates in the proliferation ratio of resting or proliferating chondrocytes at embryonic day (E) 13.5, 15.5 and 17.5, except for a small number of BrdU-negative chondrocytes at the lower zone of proliferation (see Fig. S2A,B in the supplementary material). Interestingly, however, in P3 mutant growth plates, we observed a cluster of resting-chondrocyte-like chondrocytes at the central region of growth plates that apparently lacked the ability to proliferate, in clear contrast to wild-type controls, whereas the peripheral flat-shaped proliferating chondrocytes within mutant growth plates exhibited accelerated proliferation (Fig. 3A-C). This asynchronous proliferation persisted, and at P5 these clusters of resting-chondrocyte-like chondrocytes developed into neoplastic cores. Chondrocytes within and around this core exhibited aberrant morphology and were easily distinguishable from normal chondrocytes (Fig. 3D,E). The neoplastic core was hypocellular, as indicated by enlarged, balloon-like hypoproliferating chondrocytes with a higher cytoplasm to nucleus ratio (Fig. 3F). The periphery of the neoplastic core was embedded within smaller, round chondrocytes that had a similar morphology to the resting chondrocytes (Fig. 3F). Intriguingly, we observed a small number of balloon-like chondrocytes in the lower zone of the neoplastic core that were recovering from abnormal cellularity and beginning to proliferate (Fig. 3F, yellow arrowhead).

The neoplastic core enlarged and became more distinct by P7 (Fig. 3G-I). Along with the growth and migration of the growth plate toward the epiphysis, the lower portion of the core penetrated through the hypertrophic zone into the bone marrow cavity (Fig. 3H). The non-hypertrophic chondrocytes that extended into the bone marrow cavity began to proliferate ectopically (Fig. 3I, yellow arrowhead) and to exhibit hypertrophy (Fig. 3I, red arrowhead), gradually forming a proliferating pseudo-growth plate within the bone marrow cavity (Fig. 3J-L, black arrowhead). Together, these results indicated that aberrant and asynchronous chondrocyte proliferation correlated with the initiation of dyschondroplasia in *Pten* mutant mice.

Delayed and asynchronous chondrocyte differentiation in the growth plate of *Pten* mutant mice

To determine whether aberrant proliferation in the central region of the mutant growth plates was simultaneously coupled with abnormal differentiation during the formation of the neoplastic cores, BrdU labeling-chasing experiments were used to measure the rate of differentiation of resting to proliferating chondrocytes, or of proliferating to hypertrophic chondrocytes.

In order to determine whether the chondrocytes in the neoplastic core originated from resting chondrocytes, we labeled the E15.5 cartilage primordia of growth plates with six treatments of BrdU, injected intraperitoneally into pregnant mice over 2 days. After a 7-day chase, the nuclei of the resting chondrocytes of P5.5 control tibia were still darkly stained with BrdU antibody, whereas the proliferating and hypertrophic chondrocytes were weakly or barely stained because BrdU incorporated into the genomic DNA had been diluted through the continuing division of proliferating chondrocytes (Fig. 4A). In the P5.5 mutant growth plates, a column of darkly nuclear-stained chondrocytes was observed penetrating through the middle region of the growth plate to the bone marrow cavity (Fig. 4B). The cell morphology of these BrdU-retaining chondrocytes was identical to that of chondrocytes within the neoplastic core. These BrdU labeling-chasing experiments suggested that the chondrocytes of the neoplastic core were derived from resting chondrocytes, the differentiation of which was impaired.

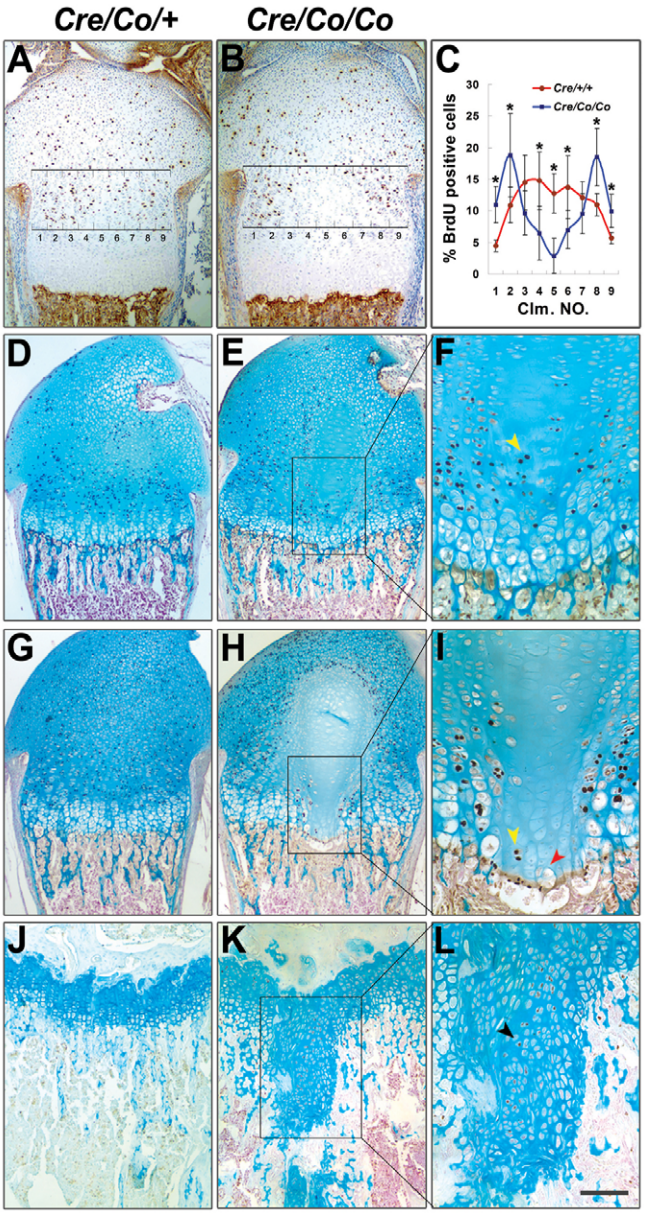

Fig. 3. Impaired, but resumable, proliferation of the center-located chondrocytes within *Pten*$^{Co/Co}$;*Col2a1-Cre* growth plates. (**A**,**B**,**D-L**) BrdU labeling was performed on sections of control (A,D,G,J) or mutant (B,E,H,K) growth plates from P3 (A,B), P5 (D,E), P7 (G,H) and P38 (J,K) mice. (**C**) The percentage of BrdU-positive chondrocytes in the proliferating zone of P3 control (A) or mutant (B) growth plates was determined in consecutive columns, as delineated by the grids, and plotted. Mean ±s.d. of six sections from three mice of each genotype. **P*<0.01. (E,H) The central region of mutant growth plate cartilage lost the ability to proliferate and gradually formed a neoplastic core. (F,I,L) Higher magnification of the boxed regions in E,H,K. Note the small number of BrdU-positive chondrocytes within the lower portion of the core (F,I, yellow arrowheads) and within the cartilaginous nodule (L, black arrowhead). Some balloon-like chondrocytes within the lower portion of the core also started to undergo hypertrophy (I, red arrowhead). Hours of BrdU labeling: A,B, 2; D,E, 5; G,H, 6; J,K, 2.5. Scale bar: 275 μm in A,B,J,K; 340 μm in D,E; 400 μm in G,H.

Additionally, in a short-term BrdU labeling-chasing experiment, after a 36-hour chase the position of the most distally located BrdU-retaining hypertrophic chondrocytes relative to the proliferating zone was closer in P1 mutant growth plates than in controls (Fig. 4C,D). Also, the BrdU-retaining hypertrophic chondrocytes that derived from proliferating chondrocytes were significantly reduced in number in mutant growth plates as compared with controls (Fig. 4C-E). These findings indicated that the hypertrophic differentiation of proliferating chondrocytes was also impaired in *Pten* mutant mice. In situ hybridization (ISH) and von-Kossa staining were performed to confirm these observations. The expression of *Ppr*, *Ihh* and *Col10a1*, which are markers for prehypertrophic and hypertrophic chondrocytes, and von-Kossa staining for terminal hypertrophic chondrocytes, were decreased in the growth plates near the neoplastic cores of P1 and P5 mutants (Fig. 4F-M; see Fig. S3K-P in the supplementary material). However, E13.5 and E16.5 mutant growth plates did not show obvious abnormalities in differentiation compared with control littermates (see Fig. S3A-J in the supplementary material). These results suggested that the successive differentiation from resting chondrocytes to terminal hypertrophic chondrocytes was delayed in the postnatal growth plates of *Pten* mutant mice, particularly within the central region where the neoplastic core was formed.

Abnormal type II collagen properties and exaggerated ER stress in *Pten* mutant mice

Histological observations suggested that matrix abnormalities were present in the neoplastic cores in *Pten* mutant mice. Therefore, we evaluated whether the properties of type II collagen (Col II; COL2; COL2α1 – Mouse Genome Informatics), the major component of collagen fibrils in the ECM secreted by chondrocytes, were altered, concurrent with the disrupted differentiation of *Pten* mutant chondrocytes. In control growth plates, the highest expression of Col II protein was detected in resting chondrocytes adjacent to the articular surface; staining became weaker at the proliferating zone (Fig. 5A,C,E, insets). In mutant growth plates, the expression of Col II fibrils in resting chondrocytes was comparable to that in controls (Fig. 5B), whereas in the neoplastic cores, abnormal properties and localization of Col II were observed (Fig. 5B). The resting-chondrocyte-like/balloon-like cells were surrounded by an extremely loose, 'empty-looking' matrix and were filled with deformed, sparse fibrils that expanded the cells and corralled the nucleus to the edge of the cytoplasm (Fig. 5D,F, insets).

Electron microscopy analyses revealed that chondrocytes from the articular surface and proliferating zone of controls exhibited intact ER and nuclear membrane (Fig. 5C,E). Additionally, resting chondrocytes were surrounded by well-formed and abundant homogenous collagen fibrils (Fig. 5C, arrowhead). Within the neoplastic core, however, collagen fibrils surrounding the chondrocytes were significantly reduced in number (Fig. 5D,F). Notably, the ER was extremely distended and fragmented (Fig. 5D,F). Procollagens were trapped in the ER and formed 'string-bead' fibrils with proteoglycan granules that were similar to those seen around the resting chondrocytes (Fig. 5C,F, arrowhead). Similar observations were made with chondrocytes cultured under conditions of oxygen tension. Under normoxic conditions, the morphology and organization of mutant chondrocytes were equivalent to those of wild-type littermates (Fig. 5G,H), as confirmed by electron microscopy (see Fig. S4A,B in the supplementary material). However, under hypoxic conditions, wild-type chondrocytes gradually formed into multiple cartilaginous nodules that were composed of chondrocytes expressing abundant Col II proteins (Fig. 5I), whereas the cultured mutant chondrocytes formed a monolayer consisting of malformed cells that were swollen by pools of Col II fibrils within the cytoplasm (Fig. 5J, arrowheads).

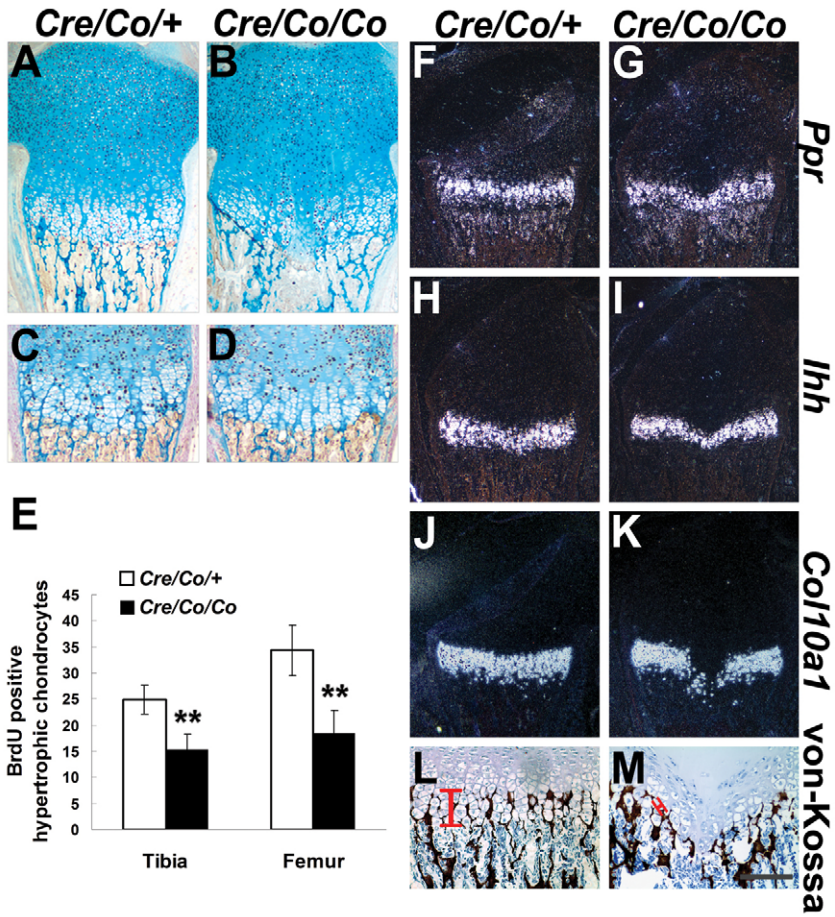

Fig. 4. Delayed and asynchronous chondrocyte differentiation within *Pten$^{Co/Co}$;Col2a1-Cre* growth plates. (**A**,**B**) Long-term BrdU labeling-chasing assay. BrdU was retained in the nuclei of resting chondrocytes and of the cells within the neoplastic core after a 7-day chase in both control (A) and mutant (B) growth plates. (**C**,**D**) Short-term BrdU labeling-chasing assay. Hypertrophic chondrocytes that transited from proliferating chondrocytes were labeled after a 1.5-day chase. (**E**) Statistical analysis of the quantities of BrdU-positive hypertrophic chondrocytes in the femur and tibia. Mean ±s.d. of six sections from two mice of each genotype. $^{**}P<0.01$. (**F-M**) Sections from P5 control (F,H,J,L) or mutant (G,I,K,M) femoral growth plate were hybridized in situ with RNA probes for *Ppr* (F,G), *Ihh* (H,I) or *Col10a1* (J,K), or subjected to von-Kossa staining (L,M). Red bars indicate layers of terminal hypertrophic chondrocytes. Scale bar: 400 μm in A,B; 275 μm in C,D,J,K; 544 μm in F-I; 222 μm in L,M.

Electron microscopy analyses demonstrated that only mutant chondrocytes cultured under hypoxia suffered greatly from a distended and fragmented ER, similar to that seen in the neoplastic cores (see Fig. S4C,D in the supplementary material).

We tracked the mRNA levels of the Col II gene (*Col2a1*) under hypoxic conditions (2% O_2) at various time points by northern blot analysis. The expression of *Col2a1* was comparable in control and mutant chondrocytes during the first 5 days of culture, indicating that *Pten* ablation did not directly influence the chondrocytic properties of the treated cells. After 7 days in culture, mutant chondrocytes in hypoxia exhibited significantly reduced *Col2a1* expression, whereas control littermates showed only mildly decreased *Col2a1* expression (Fig. 5K).

These data suggested that under conditions of PTEN deficiency, hypoxia induced severe ER stress associated with aberrant ECM properties. Nevertheless, severe ER stress failed to cause detectable apoptosis within the mutant growth plates as evaluated by TUNEL assay (see Fig. S5 in the supplementary material).

Activation of the HIF1α pathway in PTEN-deficient growth plates

That abnormalities in chondrocyte differentiation and ER function only occurred in the hypoxic portion of the cartilage suggested underlying mechanisms by which the neoplastic core was formed. The HIF1α pathway plays an essential role in avascular cartilage adaptation to hypoxia through its regulation of cell survival, cell size, ECM accumulation, blood vessel invasion and proliferation (Maes et al., 2004; Pfander et al., 2004; Schipani et al., 2001; Zelzer et al., 2004). Therefore, we performed IHC and ISH to measure the expression of HIF1α in sections from knee joints as early as E16, when the histological differences between mutants and littermate controls were not obvious, and also on sections from P1 costal and P5 femoral growth plates. In controls, HIF1α protein was abundantly expressed in the prehypertrophic/hypertrophic zone and sporadically within the central region of the resting/proliferating zone (Fig. 6A,C; see Fig. S6A in the supplementary material). By contrast, HIF1α protein levels were dramatically increased within the resting/proliferating zone of the mutant growth plate (Fig. 6B,D; see Fig. S6B in the supplementary material). Western blot analyses confirmed increased accumulation of HIF1α protein in the nuclei of mutant chondrocytes (Fig. 6E). Likewise, mRNA levels of HIF1α pathway downstream genes, *Vegf* and phosphoglycerate kinase (*Pgk*; *Pgk1*), were significantly increased in *Pten* mutants (Fig. 6F-M; see Fig. S6C-F in the supplementary material). Real-time RT-PCR verified the elevated mRNA expression of total *Vegf*, *Vegf* isoforms ($Vegf_{120}$, $Vegf_{164}$) and of *Pgk* within mutant cartilage from knee joints (Fig. 6N).

This altered HIF1α pathway activity might impact chondrocyte proliferation. We measured the expression of cyclin-dependent kinase inhibitor $p21^{Cip1}$ (CDKN1A – Mouse Genome Informatics), which has been reported to be the mediator of HIF1α-regulated growth arrest (Koshiji et al., 2004). $p21^{Cip1}$ was expressed in a manner similar to that of HIF1α, and was elevated in PTEN-deficient growth plates (Fig. 6O-R; see Fig. S6G,H in the supplementary material). $p57^{Kip2}$ (*Cdkn1c*), another cyclin-dependent kinase inhibitor that has been reported to be an effector of chondrocyte growth arrest downstream of HIF1α (Pfander et al., 2004; Schipani et al., 2001), was also upregulated in *Pten*

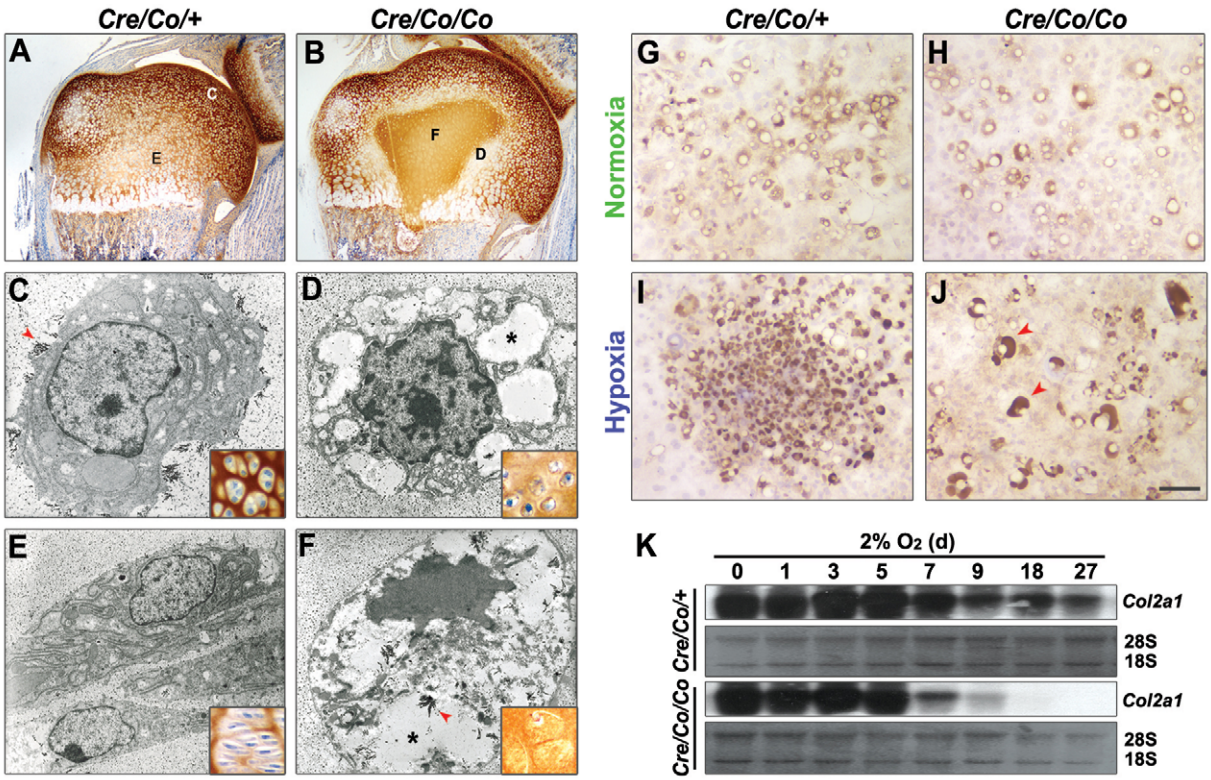

Fig. 5. Abnormal cellularity and Col II properties in *Pten*$^{Co/Co}$;*Col2a1-Cre* growth plates. (**A**,**B**) Immunohistochemistry (IHC) for type II collagen (Col II) proteins performed on mouse P5 proximal humeral growth plate sections. The neoplastic core was clearly distinguishable by its abnormal cellularity and Col II properties (B). (**C-F**) Electron microscopy images of chondrocytes and surrounding matrix from resting zone (C) and proliferating zone (E) control growth plate, or from the periphery (D) and central region (F) of the core. The insets show higher magnification views from positions indicated in A or B. The ER of the abnormal cells was extremely distended and fragmented (D,F, asterisks) compared with the normal ER (C,E). Note the premature 'string-bead' fibrils implanted inside the deformed ER (F, red arrowhead), which were similar to those surrounding the resting chondrocytes (C, red arrowhead). (**G-J**) IHC for Col II proteins of wild-type (G,I) and mutant (H,J) chondrocytes cultured under normoxic (G,H) or hypoxic (I,J) conditions. Note that *Pten* mutant chondrocytes were detached from each other and were swollen by pools of Col II fibrils within the cytoplasm under hypoxic conditions (J, red arrowheads). (**K**) *Col2a1* mRNA expression in control and mutant primary chondrocytes cultured under hypoxic conditions as evaluated by northern blot. Scale bar: 500 μm in A,B; 2 μm in C; 2.5 μm in D; 2.9 μm in E; 3.1 μm in F; 90 μm in insets, C-F; 120 μm in G-J.

mutants compared with controls (Fig. 6S-V; see Fig. S6I,J in the supplementary material). Additionally, we investigated the blood supply of the growth plate cartilage by anti-CD31 (PECAM1) whole-mount immunostaining or Hematoxylin and Eosin staining (see Fig. S7A,B,E,F in the supplementary material). Increased angiogenesis surrounding the articular surface of P3 femur (see Fig. S7C,D in the supplementary material) and an excessive invasion of blood vessels within P25 growth plate cartilage (see Fig. S7F in the supplementary material) were observed in *Pten* mutants, indicating that the HIF1α pathway activation and neoplastic core formation were not caused by poor angiogenesis in the mutant mice. Taken together, these findings strongly suggest that a lack of PTEN in chondrocytes results in the activation of the HIF1α pathway and an increase in the expression of target genes.

Overactivated HIF1α pathway accelerates ER stress in *Pten* mutant chondrocytes

To further dissect whether ER stress in *Pten* mutant chondrocytes was linked with the activated HIF1α pathway, we first evaluated by ISH the expression of the molecular chaperone, binding Ig protein (*BiP*; *Hspa5* – Mouse Genome Informatics), which is a master regulator of ER stress. At E16, abundant but equivalent *BiP* mRNA levels were detected in control and mutant growth plates through the proliferating zone (Fig. 7A,B). At P1 or P5, *BiP* mRNA was significantly upregulated in the region surrounding the neoplastic core (Fig. 7C,D; see Fig. S6K,L, arrowheads, in the supplementary material). Western blot and real-time RT-PCR analyses revealed that under hypoxia, *BiP* mRNA and protein levels increased much more rapidly in *Pten* mutant chondrocytes than in wild-type controls (Fig. 7E and data not shown).

These data indicated that overactivation of HIF1α signaling preceded the induction of ER stress and might therefore be responsible for the emergence of ER stress in *Pten* mutant chondrocytes. In order to verify this, a prolyl hydroxylase inhibitor, dimethyloxaloylglycine (DMOG), that acts to specifically stabilize HIF1α levels at normal oxygen tensions, was employed. After a 2-day culture, DMOG elevated HIF1α and downstream *Vegf* levels, as well as BiP expression, in a dose-dependent manner (Fig. 7F and data not shown). In a timecourse experiment, the activation of HIF1α by DMOG preceded upregulation of BiP (Fig. 7G), particularly in *Pten* mutant chondrocytes (Fig. 7G), suggesting that PTEN-deficient chondrocytes were more susceptible to hypoxia and subsequently suffered from ER stress.

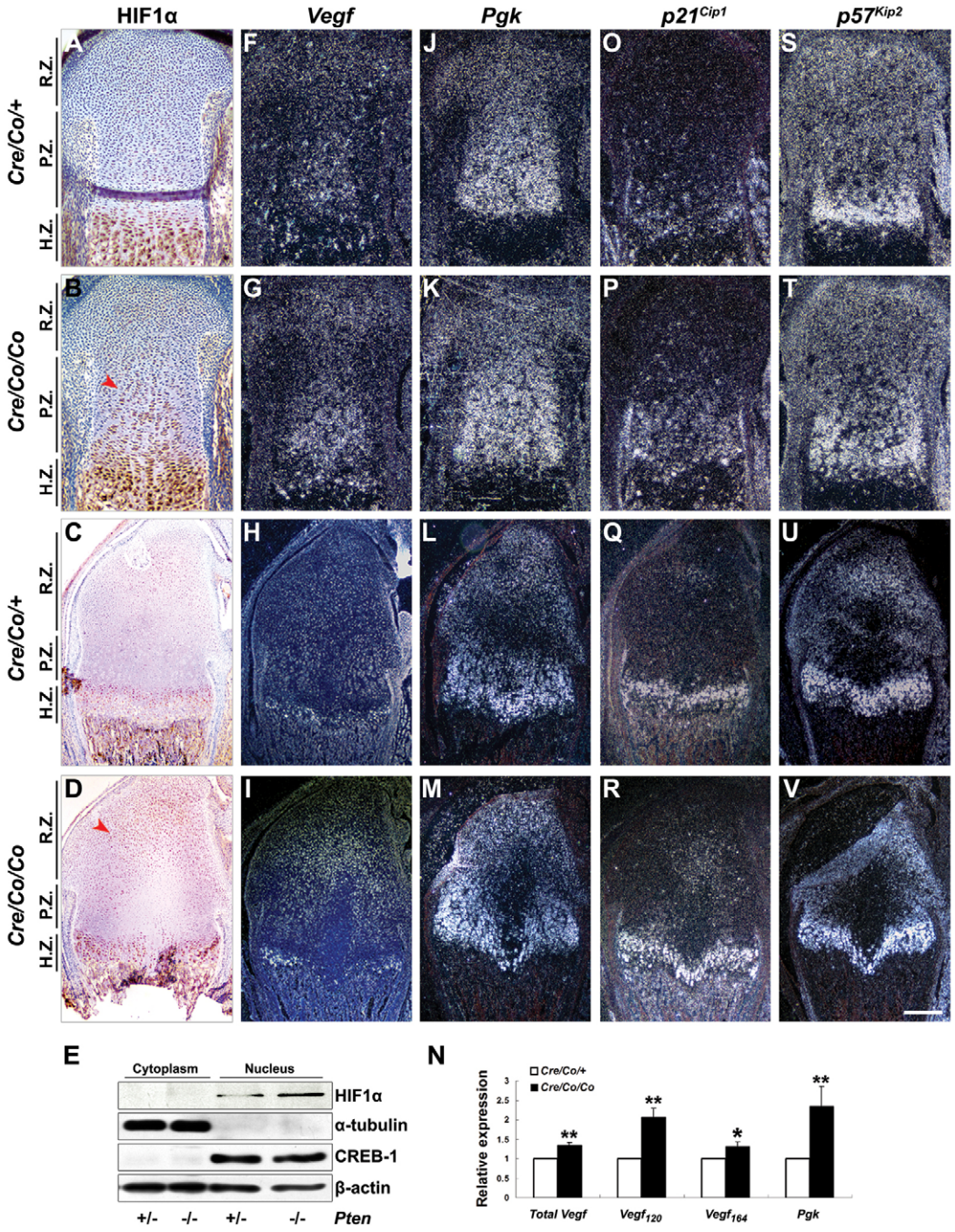

Fig. 6. Activated HIF1α pathway in *Pten$^{Co/Co}$;Col2a1-Cre* growth plates. (**A-D**,**F-M**,**O-V**) Sections of proximal tibial growth plates from E16 mouse embryos (A,B,F,G,J,K,O,P,S,T) and P5 femoral growth plates (C,D,H,I,L,M,Q,R,U,V) were subjected to IHC for HIF1α protein expression (A-D) or in situ hybridization with RNA probes for *Vegf* (F-I), *Pgk* (J-M), *p21^{Cip1}* (O-R) or *p57^{Kip2}* (S-V). Note the ectopic activation of HIF1α protein within mutant growth plates (B,D, red arrowheads). (**E**) Western blot analysis of HIF1α protein accumulation in the nuclei of control or mutant chondrocytes isolated from knee joints. (**N**) mRNA expression of total *Vegf*, *Vegf* isoforms (*Vegf$_{120}$*, *Vegf$_{164}$*) and *Pgk* within control or mutant cartilage from knee joints as revealed by real-time RT-PCR. Error bars represent means ± s.d. from six replicate PCR reactions of a single experiment.*P<0.05, **P<0.01. Scale bar: 200 μm in A,B,F,G,J,K,O,P,S,T; 470 μm in C,D,H,I,L,M,Q,R,U,V.

DISCUSSION

In the present study, we have generated chondrocyte-specific *Pten* knockout mice using the well-characterized *Col2a1-Cre* transgenic mice. Chondrocyte-specific disruption of *Pten* results in dyschondroplasia owing to interrupted proliferation and delayed differentiation of chondrocytes. This disruption correlates with an activated HIF1α pathway followed by severe ER stress, demonstrating a pivotal role for chondrocytic PTEN in endochondral ossification.

We have identified an indispensable function for PTEN in the inhibition of dyschondroplasia through its regulation of the proliferation and differentiation of chondrocytes in the growth plate. The most striking phenotype in the *Pten* mutant mice was the prevalence of cartilaginous neoplasms exhibiting pathological characteristics similar to those of human enchondromas. The neoplastic core could be observed at birth and became gradually more apparent via histology by P5. These cores continued growing and survived the zone of hypertrophy and the terminal end of the growth plate. Thereafter, the neoplastic cores were either cut off from the plates and then consumed by intramedullary tissue, or extended into metaphysis, diaphysis or epiphysis (Fig. 2B,D,F). Considering that a loss of PTEN activates PI3K/AKT, which is frequently found to be upregulated in various tumors, we expected that chondrocyte proliferation would be accelerated in *Pten* mutants. However, the proliferation of *Pten* mutant chondrocytes was in fact decreased in the neoplastic core as compared with controls (Fig. 3B,E,H). Consistent with this, a recent study observed no significant difference in chondrocyte proliferation between *Pten* knockout and

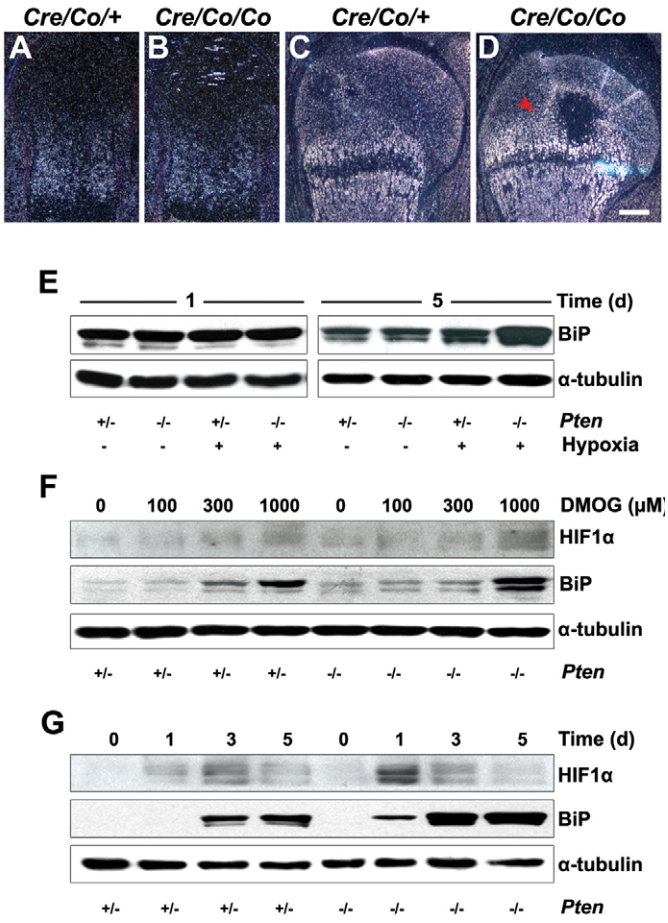

Fig. 7. Activated HIF1α pathway causes ER stress in chondrocytes. In situ hybridization for *BiP* mRNA in mouse E16 proximal tibial (**A**,**B**) and P5 proximal humeral (**C**,**D**) growth plates. Note the ectopic activation of *BiP* mRNA around the neoplastic core of mutant growth plates (D, arrowhead). (**E**) BiP protein expression in control and mutant primary chondrocytes cultured under normoxic or hypoxic conditions for 1 or 5 days as revealed by western blot analysis. (**F**) Control and mutant chondrocytes were treated with increasing concentrations of DMOG for 2 days and then analyzed by western blot with antibodies against HIF1α and BiP. (**G**) Control and mutant chondrocytes were treated with 1 mM DMOG for increasing times and then analyzed by western blot with antibodies against HIF1α and BiP. Scale bar: 200 μm in A,B; 470 μm in C,D.

control mice (Ford-Hutchinson et al., 2007), indicating that a PTEN deficiency causes dyschondroplasia through mechanisms other than increased proliferation. Importantly, here we provide compelling evidence to suggest that the dyschondroplasia in *Pten* mutant mice actually originates from resting chondrocytes, the differentiation of which was inhibited. The neoplastic chondrocytes, as well as the resting chondrocytes, were still positive for BrdU staining after a 7-day chase (Fig. 4B), indicating that the proliferation and differentiation of mutant chondrocytes in the neoplastic core were halted. The mutant chondrocytes in the neoplastic core did not show hypertrophic differentiation (Fig. 4F-M), suggesting that the terminal differentiation of these chondrocytes was also impaired. These results provide experimental support for the hypotheses that enchondromas originate from a cluster of dysplastic resting chondrocytes (Brien et al., 1997; Milgram, 1983; Potter et al., 2005).

We observed, for the first time, that resting chondrocytes surviving ER stress play a crucial role during the formation of dyschondroplasia, demonstrating the function of chondrocytic PTEN in regulating cellular responses to ER stress. Recent studies have suggested that ER stress is likely to play an important role in cartilage cell growth, differentiation and apoptosis (Yang et al., 2005). Transgenic mice carrying the mouse equivalent of a human MCDS (metaphyseal chondrodysplasia, Schmid type) p.P620fsX621 mutation, or a 13-bp deletion in *Col10a1*, harbor hypertrophic chondrocytes that suffer from dramatic ER stress and disrupted terminal differentiation (Ho et al., 2007; Tsang et al., 2007). Chondrocyte-specific *S1P* (*Mbtps1*) knockout mice exhibit chondrodysplasia and a complete lack of endochondral ossification caused by defects in Col II secretion and increased apoptosis (Patra et al., 2007). Several lines of evidence have suggested that *Pten* mutant resting chondrocytes suffer from severe ER stress. Evaluation of the ECM of the neoplastic core, including electron microscopy analyses, revealed an accumulation of Col II in the dramatically enlarged ER (Fig. 5D,F). The upregulation of *BiP*, together with the downregulation of *Ppr Ihh* and *Col10a1*, indicated that ER stress was triggered upon *Pten* deletion in chondrocytes and resulted in decreased differentiation. Interestingly, ER stress was significantly increased in *Pten* mutant chondrocytes under conditions of hypoxia, suggesting that a PTEN deficiency together with hypoxia synergistically triggers ER stress and subsequent de-differentiation of *Pten* mutant chondrocytes. According to the expression pattern of *BiP* and the TUNEL assay (Fig. 7E; see Fig. S5 in the supplementary material), hypoxia-induced ER stress in *Pten* mutants appeared to act as a mild stressor (Rutkowski et al., 2006) that chondrocytes could ultimately adapt to and survive. Furthermore, an upregulation of p-AKT in chondrocytes may be implicated in protecting cells from ER stress-induced apoptosis (Han et al., 2006; Hosoi et al., 2007; Hu et al., 2007; Matthews et al., 2007; Qu et al., 2004). The activation of HIF1α might also help chondrocytes to survive hypoxia-induced ER stress (Harding et al., 2000). Thus, the activation of the PI3K/AKT pathway in chondrocytes might serve multiple functions during the progression of hypoxia-induced ER stress; it perturbs the ER but may save the cell. As a consequence, dysplastic chondrocytes develop.

We provide convincing evidence that the HIF1α pathway is involved in the formation of neoplastic cores in *Pten* mutant mice. Previous studies have shown that the HIF1α/VEGF pathway plays essential roles in the ability of avascular cartilage to adapt to hypoxia (Schipani, 2005). Inactivation of HIF1α in chondrocytes leads to increased cell death, accelerated proliferation and reduced yield of *Vegf*, *Pgk* and $p57^{Kip2}$ (Schipani et al., 2001). Loss-of-function studies with *Vegf* and its derivative isoforms have confirmed their roles in cell survival, blood vessel invasion and proliferation (Maes et al., 2002; Maes et al., 2004; Zelzer et al., 2004; Zelzer et al., 2002). By contrast, inactivation of murine von Hippel-Lindau tumor suppressor protein (VHL) in chondrocytes causes enlarged cell size, accumulation of ECM, decreased proliferation and increased expression of *Vegf*, *Pgk* and $p57^{Kip2}$ through a mechanism that facilitates the stabilization and accumulation of HIF1α protein (Pfander et al., 2004). Several in vitro studies have implicated PI3K/AKT signaling in regulating the HIF1α/VEGF pathway. Hypoxia can directly induce the activation of AKT and might also induce the activity of HIF1α via AKT (Emerling et al., 2008; Li et al., 2005; Pore et al., 2006; Zundel et al., 2000). Activation of AKT can increase HIF1α and VEGF expression in various cancer cell lines (Blancher et al.,

2001; Mottet et al., 2003; Skinner et al., 2004). In the present study, we demonstrate that activation of AKT caused by loss of PTEN in chondrocytes leads to an upregulation of HIF1α and its downstream targets, *Vegf* and *Pgk*, at E16, when the neoplastic core has not yet formed in *Pten* mutants. Activation of HIF1α also brought on an increase in $p21^{Cip1}$ and $p57^{Kip2}$ expression, which might contribute to the decreased proliferation observed in the neoplastic cores (Dang et al., 2008; Gordan et al., 2007; Koshiji et al., 2004; Schipani et al., 2001). Importantly, a synergistic role of the PI3K/AKT and HIF1α pathways in inducing ER stress in chondrocytes was observed. We found that overactivated HIF1α signaling could trigger ER stress in chondrocytes and, interestingly, that deletion of *Pten* enhanced HIF1α signaling and accelerated the course and severity of ER stress. These findings provided in vivo evidence that PTEN modulates chondrocyte adaptation to hypoxia via inhibition of the HIF1α pathway and ER stress signaling. However, whether PTEN deficiency under hypoxia induces altered protein secretion, which might then lead to the activation of ER stress, remains to be clarified.

Altogether, these observations suggest that the activation of AKT through a loss of PTEN function leads to the activation of the HIF1α pathway and, consequently, to prolonged ER stress, which respectively block the proliferation and differentiation of the mutant chondrocytes, resulting in dyschondroplasia.

We thank Tak Wah Mak for *Pten* conditional knockout mice; Ernestina Schipani for in situ hybridization probes for *Col2a1*, $p57^{Kip2}$, *Pgk* and *Vegf*; Bin Liu for Col II antibody; Ming Fan, Fanwei Meng, Youliang Wang, Xinlong Yan, Hua Zhao and Xin Huang for technical support and helpful discussion. The mouse anti-Col II antibody was obtained from the Developmental Studies Hybridoma Bank developed under the auspices of the NICHD and maintained by The University of Iowa. This work was supported by the Chinese National Key Program on Basic Research (2005CB522506, 2006CB943501, 2006BAI23B01-3), National Natural Science Foundation of China (30430350), National High-Tech Research and Development Program (2006AA02Z168) and grants from Beijing Municipal Science Technology Commission (H030230280410; Z0006303041231).

Supplementary material

Supplementary material for this article is available at http://dev.biologists.org/cgi/content/full/135/21/3587/DC1

References

Ayala, G., Liu, C., Nicosia, R., Horowitz, S. and Lackman, R. (2000). Microvasculature and VEGF expression in cartilaginous tumors. *Hum. Pathol.* **31**, 341-346.

Backman, S. A., Stambolic, V., Suzuki, A., Haight, J., Elia, A., Pretorius, J., Tsao, M. S., Shannon, P., Bolon, B., Ivy, G. O. et al. (2001). Deletion of Pten in mouse brain causes seizures, ataxia and defects in soma size resembling Lhermitte-Duclos disease. *Nat. Genet.* **29**, 396-403.

Blancher, C., Moore, J. W., Robertson, N. and Harris, A. L. (2001). Effects of ras and von Hippel-Lindau (VHL) gene mutations on hypoxia-inducible factor (HIF)-1alpha, HIF-2alpha, and vascular endothelial growth factor expression and their regulation by the phosphatidylinositol 3′-kinase/Akt signaling pathway. *Cancer Res.* **61**, 7349-7355.

Brien, E. W., Mirra, J. M. and Kerr, R. (1997). Benign and malignant cartilage tumors of bone and joint: their anatomic and theoretical basis with an emphasis on radiology, pathology and clinical biology. I. the intramedullary cartilage tumors. *Skeletal Radiol.* **26**, 325-353.

Chow, L. M. and Baker, S. J. (2006). PTEN function in normal and neoplastic growth. *Cancer Lett.* **241**, 184-196.

Cully, M., You, H., Levine, A. J. and Mak, T. W. (2006). Beyond PTEN mutations: the PI3K pathway as an integrator of multiple inputs during tumorigenesis. *Nat. Rev. Cancer* **6**, 184-192.

Dang, C. V., Kim, J. W., Gao, P. and Yustein, J. (2008). The interplay between MYC and HIF in cancer. *Nat. Rev. Cancer* **8**, 51-56.

Emerling, B. M., Weinberg, F., Liu, J. L., Mak, T. W. and Chandel, N. S. (2008). PTEN regulates p300-dependent hypoxia-inducible factor 1 transcriptional activity through Forkhead transcription factor 3a (FOXO3a). *Proc. Natl. Acad. Sci. USA* **105**, 2622-2627.

Ford-Hutchinson, A. F., Ali, Z., Lines, S. E., Hallgrimsson, B., Boyd, S. K. and Jirik, F. R. (2007). Inactivation of Pten in osteo-chondroprogenitor cells leads to epiphyseal growth plate abnormalities and skeletal overgrowth. *J. Bone Miner. Res.* **22**, 1245-1259.

Gordan, J. D., Thompson, C. B. and Simon, M. C. (2007). HIF and c-Myc: sibling rivals for control of cancer cell metabolism and proliferation. *Cancer Cell* **12**, 108-113.

Han, S., Liang, C. P., DeVries-Seimon, T., Ranalletta, M., Welch, C. L., Collins-Fletcher, K., Accili, D., Tabas, I. and Tall, A. R. (2006). Macrophage insulin receptor deficiency increases ER stress-induced apoptosis and necrotic core formation in advanced atherosclerotic lesions. *Cell Metab.* **3**, 257-266.

Harding, H. P., Zhang, Y., Bertolotti, A., Zeng, H. and Ron, D. (2000). Perk is essential for translational regulation and cell survival during the unfolded protein response. *Mol. Cell* **5**, 897-904.

Hashimoto, Y., Tomiyama, T., Yamano, Y. and Mori, H. (2003). Mutation (D472Y) in the type 3 repeat domain of cartilage oligomeric matrix protein affects its early vesicle trafficking in endoplasmic reticulum and induces apoptosis. *Am. J. Pathol.* **163**, 101-110.

Ho, M. S., Tsang, K. Y., Lo, R. L., Susic, M., Makitie, O., Chan, T. W., Ng, V. C., Sillence, D. O., Boot-Handford, R. P., Gibson, G. et al. (2007). COL10A1 nonsense and frame-shift mutations have a gain-of-function effect on the growth plate in human and mouse metaphyseal chondrodysplasia type Schmid. *Hum. Mol. Genet.* **16**, 1201-1215.

Hopyan, S., Gokgoz, N., Poon, R., Gensure, R. C., Yu, C., Cole, W. G., Bell, R. S., Juppner, H., Andrulis, I. L., Wunder, J. S. et al. (2002). A mutant PTH/PTHrP type I receptor in enchondromatosis. *Nat. Genet.* **30**, 306-310.

Hosoi, T., Hyoda, K., Okuma, Y., Nomura, Y. and Ozawa, K. (2007). Akt up- and down-regulation in response to endoplasmic reticulum stress. *Brain Res.* **1152**, 27-31.

Hu, M. C., Gong, H. Y., Lin, G. H., Hu, S. Y., Chen, M. H., Huang, S. J., Liao, C. F. and Wu, J. L. (2007). XBP-1, a key regulator of unfolded protein response, activates transcription of IGF1 and Akt phosphorylation in zebrafish embryonic cell line. *Biochem. Biophys. Res. Commun.* **359**, 778-783.

Kalinski, T., Krueger, S., Sel, S., Werner, K., Ropke, M. and Roessner, A. (2006). Differential expression of VEGF-A and angiopoietins in cartilage tumors and regulation by interleukin-1beta. *Cancer* **106**, 2028-2038.

Karsenty, G. and Wagner, E. F. (2002). Reaching a genetic and molecular understanding of skeletal development. *Dev. Cell* **2**, 389-406.

Koshiji, M., Kageyama, Y., Pete, E. A., Horikawa, I., Barrett, J. C. and Huang, L. E. (2004). HIF-1alpha induces cell cycle arrest by functionally counteracting Myc. *EMBO J.* **23**, 1949-1956.

Kronenberg, H. M. (2003). Developmental regulation of the growth plate. *Nature* **423**, 332-336.

Kunisada, T., Moseley, J. M., Slavin, J. L., Martin, T. J. and Choong, P. F. (2002). Co-expression of parathyroid hormone-related protein (PTHrP) and PTH/PTHrP receptor in cartilaginous tumours: a marker for malignancy? *Pathology* **34**, 133-137.

Lan, Y., Liu, B., Yao, H., Li, F., Weng, T., Yang, G., Li, W., Cheng, X., Mao, N. and Yang, X. (2007). Essential role of endothelial Smad4 in vascular remodeling and integrity. *Mol. Cell. Biol.* **27**, 7683-7692.

Li, Y. M., Zhou, B. P., Deng, J., Pan, Y., Hay, N. and Hung, M. C. (2005). A hypoxia-independent hypoxia-inducible factor-1 activation pathway induced by phosphatidylinositol-3 kinase/Akt in HER2 overexpressing cells. *Cancer Res.* **65**, 3257-3263.

Maes, C., Carmeliet, P., Moermans, K., Stockmans, I., Smets, N., Collen, D., Bouillon, R. and Carmeliet, G. (2002). Impaired angiogenesis and endochondral bone formation in mice lacking the vascular endothelial growth factor isoforms VEGF164 and VEGF188. *Mech. Dev.* **111**, 61-73.

Maes, C., Stockmans, I., Moermans, K., Van Looveren, R., Smets, N., Carmeliet, P., Bouillon, R. and Carmeliet, G. (2004). Soluble VEGF isoforms are essential for establishing epiphyseal vascularization and regulating chondrocyte development and survival. *J. Clin. Invest.* **113**, 188-199.

Matthews, J. A., Belof, J. L., Acevedo-Duncan, M. and Potter, R. L. (2007). Glucosamine-induced increase in Akt phosphorylation corresponds to increased endoplasmic reticulum stress in astroglial cells. *Mol. Cell. Biochem.* **298**, 109-123.

McGough, R. L., Lin, C., Meitner, P., Aswad, B. I. and Terek, R. M. (2002). Angiogenic cytokines in cartilage tumors. *Clin. Orthop. Relat. Res.* **397**, 62-69.

Milgram, J. W. (1983). The origins of osteochondromas and enchondromas. A histopathologic study. *Clin. Orthop. Relat. Res.* **174**, 264-284.

Mottet, D., Dumont, V., Deccache, Y., Demazy, C., Ninane, N., Raes, M. and Michiels, C. (2003). Regulation of hypoxia-inducible factor-1alpha protein level during hypoxic conditions by the phosphatidylinositol 3-kinase/Akt/glycogen synthase kinase 3beta pathway in HepG2 cells. *J. Biol. Chem.* **278**, 31277-31285.

Nakase, T., Myoui, A., Shimada, K., Kuriyama, K., Joyama, S., Miyaji, T., Tomita, T. and Yoshikawa, H. (2001). Involvement of BMP-2 signaling in a cartilage cap in osteochondroma. *J. Orthop. Res.* **19**, 1085-1088.

Oliver, B. L., Cronin, C. G., Zhang-Benoit, Y., Goldring, M. B. and Tanzer, M. L. (2005). Divergent stress responses to IL-1beta, nitric oxide, and tunicamycin by chondrocytes. *J. Cell Physiol.* **204**, 45-50.

Patra, D., Xing, X., Davies, S., Bryan, J., Franz, C., Hunziker, E. B. and Sandell, L. J. (2007). Site-1 protease is essential for endochondral bone formation in mice. *J. Cell Biol.* **179**, 687-700.
Pfander, D., Kobayashi, T., Knight, M. C., Zelzer, E., Chan, D. A., Olsen, B. R., Giaccia, A. J., Johnson, R. S., Haase, V. H. and Schipani, E. (2004). Deletion of Vhlh in chondrocytes reduces cell proliferation and increases matrix deposition during growth plate development. *Development* **131**, 2497-2508.
Pirog-Garcia, K. A., Meadows, R. S., Knowles, L., Heinegard, D., Thornton, D. J., Kadler, K. E., Boot-Handford, R. P. and Briggs, M. D. (2007). Reduced cell proliferation and increased apoptosis are significant pathological mechanisms in a murine model of mild pseudoachondroplasia resulting from a mutation in the C-terminal domain of COMP. *Hum. Mol. Genet.* **16**, 2072-2088.
Pore, N., Jiang, Z., Shu, H. K., Bernhard, E., Kao, G. D. and Maity, A. (2006). Akt1 activation can augment hypoxia-inducible factor-1alpha expression by increasing protein translation through a mammalian target of rapamycin-independent pathway. *Mol. Cancer Res.* **4**, 471-479.
Potter, B. K., Freedman, B. A., Lehman, R. A., Jr, Shawen, S. B., Kuklo, T. R. and Murphey, M. D. (2005). Solitary epiphyseal enchondromas. *J. Bone Joint Surg. Am.* **87**, 1551-1560.
Qu, L., Huang, S., Baltzis, D., Rivas-Estilla, A. M., Pluquet, O., Hatzoglou, M., Koumenis, C., Taya, Y., Yoshimura, A. and Koromilas, A. E. (2004). Endoplasmic reticulum stress induces p53 cytoplasmic localization and prevents p53-dependent apoptosis by a pathway involving glycogen synthase kinase-3beta. *Genes Dev.* **18**, 261-277.
Robinson, D., Hasharoni, A., Oganesian, A., Sandell, L. J., Yayon, A. and Nevo, Z. (2001). Role of FGF9 and FGF receptor 3 in osteochondroma formation. *Orthopedics* **24**, 783-787.
Rozeman, L. B., Hameetman, L., Cleton-Jansen, A. M., Taminiau, A. H., Hogendoorn, P. C. and Bovee, J. V. (2005). Absence of IHH and retention of PTHrP signalling in enchondromas and central chondrosarcomas. *J. Pathol.* **205**, 476-482.
Rutkowski, D. T., Arnold, S. M., Miller, C. N., Wu, J., Li, J., Gunnison, K. M., Mori, K., Sadighi Akha, A. A., Raden, D. and Kaufman, R. J. (2006). Adaptation to ER stress is mediated by differential stabilities of pro-survival and pro-apoptotic mRNAs and proteins. *PLoS Biol.* **4**, e374.
Schipani, E. (2005). Hypoxia and HIF-1 alpha in chondrogenesis. *Semin. Cell Dev. Biol.* **16**, 539-546.
Schipani, E., Ryan, H. E., Didrickson, S., Kobayashi, T., Knight, M. and Johnson, R. S. (2001). Hypoxia in cartilage: HIF-1alpha is essential for chondrocyte growth arrest and survival. *Genes Dev.* **15**, 2865-2876.
Skinner, H. D., Zheng, J. Z., Fang, J., Agani, F. and Jiang, B. H. (2004). Vascular endothelial growth factor transcriptional activation is mediated by hypoxia-inducible factor 1alpha, HDM2, and p70S6K1 in response to phosphatidylinositol 3-kinase/AKT signaling. *J. Biol. Chem.* **279**, 45643-45651.
Sulzbacher, I., Birner, P., Trieb, K., Muhlbauer, M., Lang, S. and Chott, A. (2001). Platelet-derived growth factor-alpha receptor expression supports the growth of conventional chondrosarcoma and is associated with adverse outcome. *Am. J. Surg. Pathol.* **25**, 1520-1527.
Sun, Q., Zhang, Y., Yang, G., Chen, X., Zhang, Y., Cao, G., Wang, J., Sun, Y., Zhang, P., Fan, M. et al. (2008). Transforming growth factor-b-regulated miR-24 promotes skeletal muscle differentiation. *Nucleic Acids Res.* **36**, 2690-2699.
Tan, X., Weng, T., Zhang, J., Wang, J., Li, W., Wan, H., Lan, Y., Cheng, X., Hou, N., Liu, H. et al. (2007). Smad4 is required for maintaining normal murine postnatal bone homeostasis. *J. Cell Sci.* **120**, 2162-2170.
Tiet, T. D., Hopyan, S., Nadesan, P., Gokgoz, N., Poon, R., Lin, A. C., Yan, T., Andrulis, I. L., Alman, B. A. and Wunder, J. S. (2006). Constitutive hedgehog signaling in chondrosarcoma up-regulates tumor cell proliferation. *Am. J. Pathol.* **168**, 321-330.
Tsang, K. Y., Chan, D., Cheslett, D., Chan, W. C., So, C. L., Melhado, I. G., Chan, T. W., Kwan, K. M., Hunziker, E. B., Yamada, Y. et al. (2007). Surviving endoplasmic reticulum stress is coupled to altered chondrocyte differentiation and function. *PLoS Biol.* **5**, e44.
Vranka, J., Mokashi, A., Keene, D. R., Tufa, S., Corson, G., Sussman, M., Horton, W. A., Maddox, K., Sakai, L. and Bachinger, H. P. (2001). Selective intracellular retention of extracellular matrix proteins and chaperones associated with pseudoachondroplasia. *Matrix Biol.* **20**, 439-450.
Waite, K. A. and Eng, C. (2002). Protean PTEN: form and function. *Am. J. Hum. Genet.* **70**, 829-844.
Yang, L., Carlson, S. G., McBurney, D. and Horton, W. E., Jr (2005). Multiple signals induce endoplasmic reticulum stress in both primary and immortalized chondrocytes resulting in loss of differentiation, impaired cell growth, and apoptosis. *J. Biol. Chem.* **280**, 31156-31165.
Yang, L., McBurney, D., Tang, S. C., Carlson, S. G. and Horton, W. E., Jr (2007). A novel role for Bcl-2 associated-athanogene-1 (Bag-1) in regulation of the endoplasmic reticulum stress response in mammalian chondrocytes. *J. Cell. Biochem.* **102**, 786-800.
Zelzer, E., McLean, W., Ng, Y. S., Fukai, N., Reginato, A. M., Lovejoy, S., D'Amore, P. A. and Olsen, B. R. (2002). Skeletal defects in VEGF(120/120) mice reveal multiple roles for VEGF in skeletogenesis. *Development* **129**, 1893-1904.
Zelzer, E., Mamluk, R., Ferrara, N., Johnson, R. S., Schipani, E. and Olsen, B. R. (2004). VEGFA is necessary for chondrocyte survival during bone development. *Development* **131**, 2161-2171.
Zhang, J., Tan, X., Li, W., Wang, Y., Wang, J., Cheng, X. and Yang, X. (2005). Smad4 is required for the normal organization of the cartilage growth plate. *Dev. Biol.* **284**, 311-322.
Zundel, W., Schindler, C., Haas-Kogan, D., Koong, A., Kaper, F., Chen, E., Gottschalk, A. R., Ryan, H. E., Johnson, R. S., Jefferson, A. B. et al. (2000). Loss of PTEN facilitates HIF-1-mediated gene expression. *Genes Dev.* **14**, 391-396.
Zuscik, M. J., Hilton, M. J., Zhang, X., Chen, D. and O'Keefe, R. J. (2008). Regulation of chondrogenesis and chondrocyte differentiation by stress. *J. Clin. Invest.* **118**, 429-438.